

3.2. Irradiance based model

This model is appropriate for a single higher order mode polarized orthogonal to the fundamental mode. The irradiance profile is used in the steady state expression for the upper state population fraction,

$$n_u(x,y) = \frac{P_p \sigma_p^a / h\nu_p A + I_s \sigma_s^a / h\nu_s}{P_p(\sigma_p^a + \sigma_p^e) / h\nu_p A + I_s(\sigma_s^a + \sigma_s^e) / h\nu_s + 1/\tau}, \quad (1)$$

to compute the upper state profile across the fiber at each z location. Here P_p is the pump power, σ_p^a is the pump absorption cross section, σ_p^e is the pump emission cross section, σ_s^a is the signal absorption cross section, σ_s^e is the signal emission cross section, A is the pump cladding area, I_s is the signal irradiance formed by adding the irradiances of the signal modes, and τ is the upper state radiative lifetime. The irradiance profile I_s is computed by adding the irradiance profiles of the two modes. We use the usual approximation that the pump light is uniformly distributed across the pump cladding including the core. When $I_s = 0$ the upper state fraction is approximately 0.5 in amplifiers strongly pumped with 976 nm light. When $I_s \approx P_p(\sigma_p^a + \sigma_p^e)/(A\sigma_s^e)$ the upper state fraction is reduced to approximately 0.25. This reduction in n_u results in gain saturation, and this value of I_s indicates the signal level associated with saturation. Note that it is proportional to the local value of the pump power P_p .

The upper state population computed from Eq. (1) is used to compute the change in pump power using

$$\frac{dP_p}{dz} = \frac{P_p}{A} \int (\sigma_p^e n_u - \sigma_p^a n_l) N_{Yb} dx dy, \quad (2)$$

where

$$n_l = 1 - n_u. \quad (3)$$

It is also used to compute the change in signal modal powers using

$$\frac{dP_s^m}{dz} = P_s^m \int (\sigma_s^e n_u - \sigma_s^a n_l) N_{Yb} \Phi^m dx dy, \quad (4)$$

where Φ^m is the irradiance spatial profile of mode m , normalized to 1 W. The modal profiles Φ^m are not allowed to change, only the modal powers P_s^m evolve. This model runs in a few seconds.

3.3. Field based models

To include modal interference we use a split-step beam propagation method (BPM) to model the evolution of the modes. The first half of the split step is propagation of the total signal field over one dz step using FFT methods. The second half adds the phase due to the refractive index profile of the fiber, including bending, over the dz step. The second half also includes computation of the signal gain. To compute the gain the steady state upper level population is computed using Eq. (1), where I_s is computed from the square of the full optical field rather than from the sum of the irradiances of the individual modes. From n_u the gain/loss of the signal field is computed and added to the propagating field. We compute the modal content of the signal field at regular intervals along the fiber by computing the overlap integral of the propagating field with the modal fields of interest. The pump wave is propagated in the same way as in the previous model. This model runs in approximately 100 minutes.

3.4. Modeling notes

To allay doubts whether the first modeling method correctly models orthogonally polarized modes, we validated it by modeling the amplifier using the BPM model with the two orthogonally polarized modes propagated separately so there is no interference between them. The

upper state population was computed from the pump irradiance and sum of the irradiances of the two oppositely polarized signal fields. We found negligible difference between this and the irradiance based model. We use the same two-field BPM model to simulate a non-PM fiber by periodically swapping the two orthogonally polarized higher order mode fields. First one field and then the other interferes with the fundamental mode. We do not claim this is necessarily a realistic treatment. It treats the limiting case of a large difference in the birefringence of the fundamental and higher order mode, which is useful given our lack of detailed knowledge of actual polarization evolution.

We verified convergence of the models by doubling the grid resolution in each of the dimensions, x , y , (from $1.2 \times 1.2 \mu\text{m}$) and z (from $2 \mu\text{m}$). We also verified that mixtures of modes propagate as expected if the doping concentration is set to zero, or if the pump power is set to zero.

We also showed that doubling the doping density while keeping the amplifier length constant was nearly equivalent to keeping the doping constant and doubling the length. This is used below to facilitate modeling of restricted area doping.

In our earlier paper [1] we argued and demonstrated that stationary refractive index gratings caused by spatial hole burning, either through the Kramers-Kronig effect or through nonuniform heating, cannot cause power transfer between modes. Indeed, when we included such refractive index changes in our BPM models, we found no significant difference from the results without them. Therefore refractive index changes associated with modal interference are not included in the modeling results presented here.

4. Modeled amplifier performance

In the following subsections we present model results for straight and bent fiber with different doping diameters, from full core to one third of the core. We believe the trends are quite clear from the limited number of examples we can present here.

For later comparisons we present in Fig. 2 the baseline performance of co- and counter-pumped, straight, fully doped, amplifiers with the parameters of Table 1. The power in all higher order modes is zero.

4.1. Full core doping

Our first example clearly illustrates the difference between the behavior of higher order modes of parallel and orthogonal polarizations. Mode competition suppresses the growth of the \parallel polarized modes relative to the strong fundamental mode, but enhances the growth of the \perp polarized modes. Fig. 3 shows plots of the power in modes $m_{2\parallel}$ and $m_{2\perp}$ relative to the m_1 power, for a co-pumped amplifier (top) and for a counter-pumped amplifier (bottom). The power in m_2 is initially 1% of the power in m_1 . The irradiance based model is used to compute $m_{2\perp}$, while the field based BPM model is used for $m_{2\parallel}$ and for non-PM fiber. Because our model for non-PM fiber switches the polarization many times at regular intervals, the light in either polarization state at any position has propagated nearly equal distances in each polarization state. This implies the non-PM curve should approximate the geometric mean of the parallel and orthogonal curves, and we verified this.

In the co-pumped case most of the separation in power between $m_{2\parallel}$ and $m_{2\perp}$ occurs before $z = 2 \text{ m}$. For greater distances the pump is weak and the signal strong (see upper plot in Fig. 2) so the upper state population is strongly suppressed across the full core, and m_2 with either polarization experiences approximately the same gain as m_1 . In the counter-pumped case the separation between $m_{2\perp}$ and $m_{2\parallel}$ continues to grow over the full length of the fiber because the signal and pump powers are comparable the whole way, causing a relatively constant, moderate gain saturation.

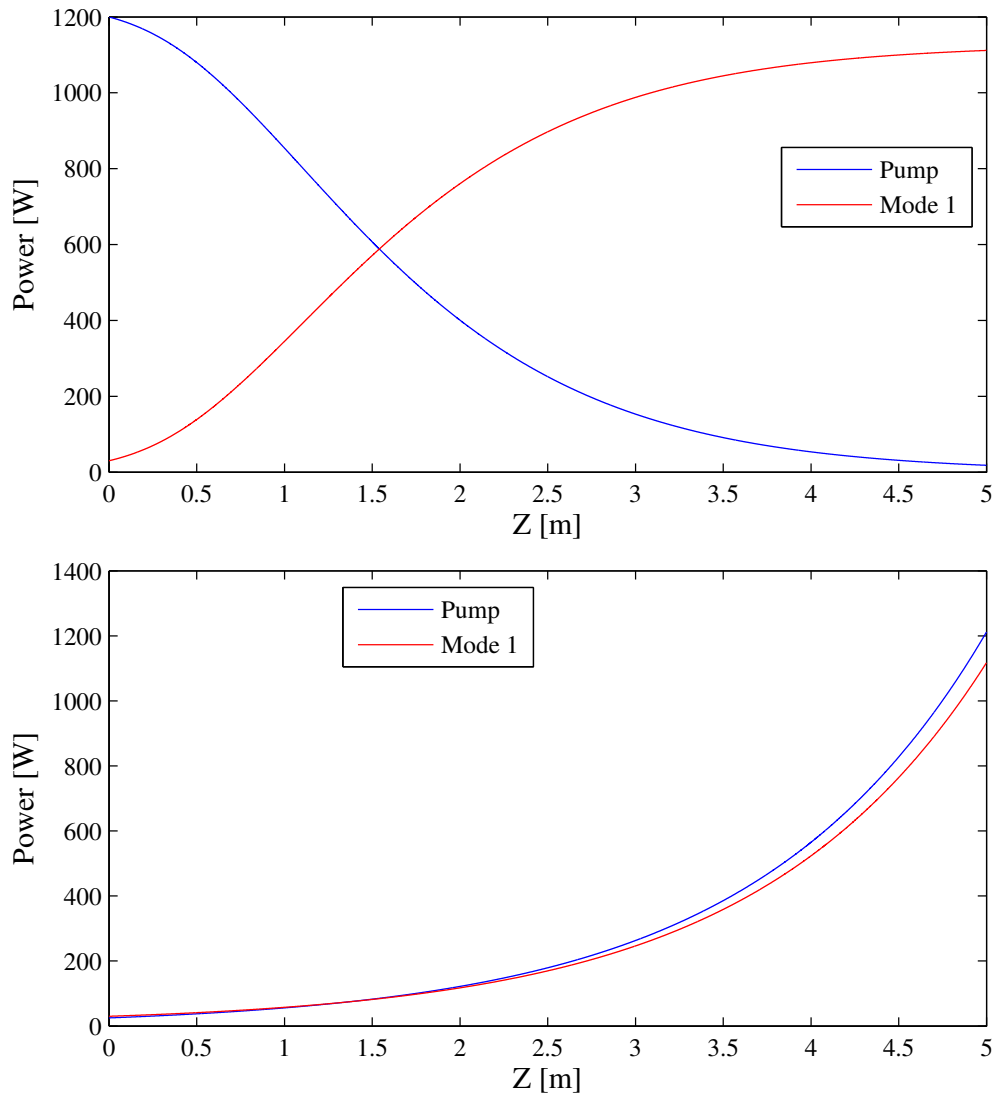


Fig. 2. Baseline model results for co-pumped amplifier (top) and counter-pumped amplifier (bottom) using the parameters in Table 1. Higher order modal input powers are set to zero.

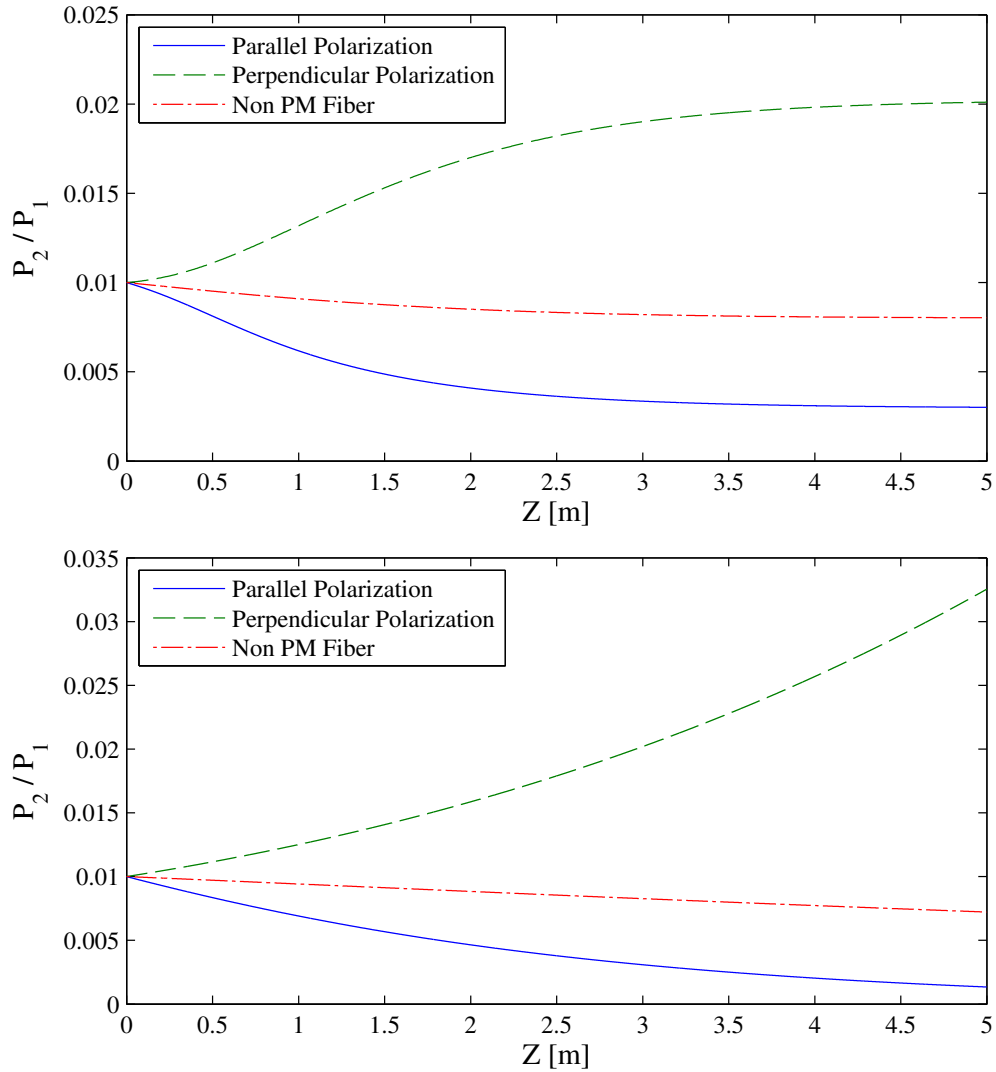


Fig. 3. Power in $m_{2\parallel}$ (solid) or $m_{2\perp}$ (dashed) or the sum of $m_{2\parallel}$ and $m_{2\perp}$ (chain) divided by power in m_1 for a co-pumped amplifier (top) and a counter-pumped amplifier (bottom). The fiber is straight and the full core is doped. For the non-PM fiber the m_2 power is launched half in each polarization, and the fields for the two polarizations of m_2 are swapped every 20 mm. Other properties are listed in Table 1 and Fig. 1, and the pump and m_1 powers are nearly identical to those in Fig. 2.

At this point a physical explanation for the difference in gains of the two polarizations is called for. The cause of gain enhancement of $m_{2\perp}$ is fairly obvious. The strong m_1 depletes the gain in the center of the core where it is strongest. Mode m_2 is weak near the center but strong farther from the core center where depletion is weaker. Consequently $m_{2\perp}$ is less sensitive to the gain saturation than m_1 , so it has higher gain than m_1 . The suppression of $m_{2\parallel}$ must be related to its interference with m_1 . When the phase between m_1 and $m_{2\parallel}$ is $\pi/2$, there is no interference, and the situation is exactly the same as for $m_{2\perp}$, so $m_{2\parallel}$ has higher gain than mode one. However, when the phase between the modes is zero, the irradiance profile is asymmetric in the plane of the lobes of m_2 . On one side the fields of m_1 and $m_{2\parallel}$ interfere constructively, on the other destructively. Gain is higher on the destructive side due to a less depleted upper state population there, so that side of the field grows more there than the opposite. The result is a symmetrization of the field across the core. Although it might not be readily apparent, modal decomposition shows that this is equivalent to the suppression of m_2 relative to m_1 . So, depending on the relative phases of the two modes, m_2 is either enhanced or suppressed. In all the cases we have modeled the suppression is stronger than the enhancement, with the net result being mode suppression. This phase sensitivity is apparent in the magnified plot of the m_2 power divided by the m_1 power shown in Fig. 4. As expected, the oscillation period is half the mode beat length, with growth and suppression behaving exactly as we just described.

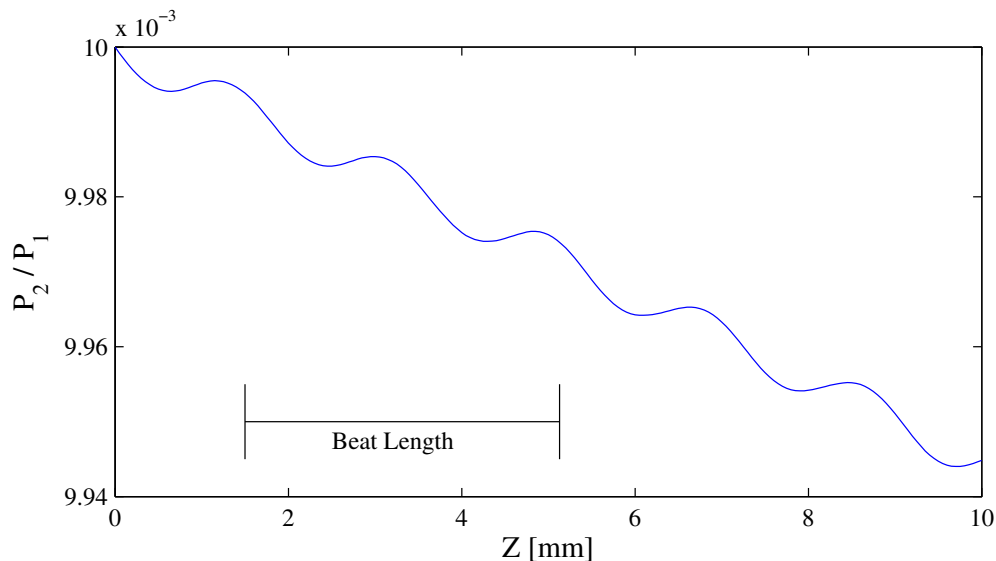


Fig. 4. Ratio of power in $m_{2\parallel}$ to power in m_1 for $P_s^1 = 300$ W and $P_s^2 = 3$ W. The beat length is 3.63 mm for these two modes. Depending on the phase between the two modes, $m_{2\parallel}$ growth relative to m_1 is either positive or negative, but the net change in this ratio over a full cycle is negative.

4.2. Confined doping

One widely discussed method of improving modal purity is to confine the doping to a central portion of the core [5, 6, 8–10, 15]. This improves the overlap of the gain with the fundamental mode relative to the higher order modes. We test this using our models, increasing doping concentration as necessary to maintain constant pump absorption.

Fig. 5 summarizes our results for m_2 (top) and m_6 (bottom) in unbent fiber. The gain G_m is

defined as the output power of mode m divided by its input power. The doping diameter is varied from $10\ \mu\text{m}$ up to the full core diameter of $30\ \mu\text{m}$. As expected, the gain of $m_{2\perp}$ can be reduced below that of the fundamental by reducing the doping diameter below $24\ \mu\text{m}$. Similarly, the gain of $m_{6\perp}$ can be reduced below the fundamental by reducing the doping diameter below $28\ \mu\text{m}$. One important point is that, according to these plots, confined doping influences the \parallel polarized modes in nearly the same way as the \perp modes. The curves for a non-PM fiber in all four graphs can be estimated by taking the geometric mean of the parallel and orthogonal curves.

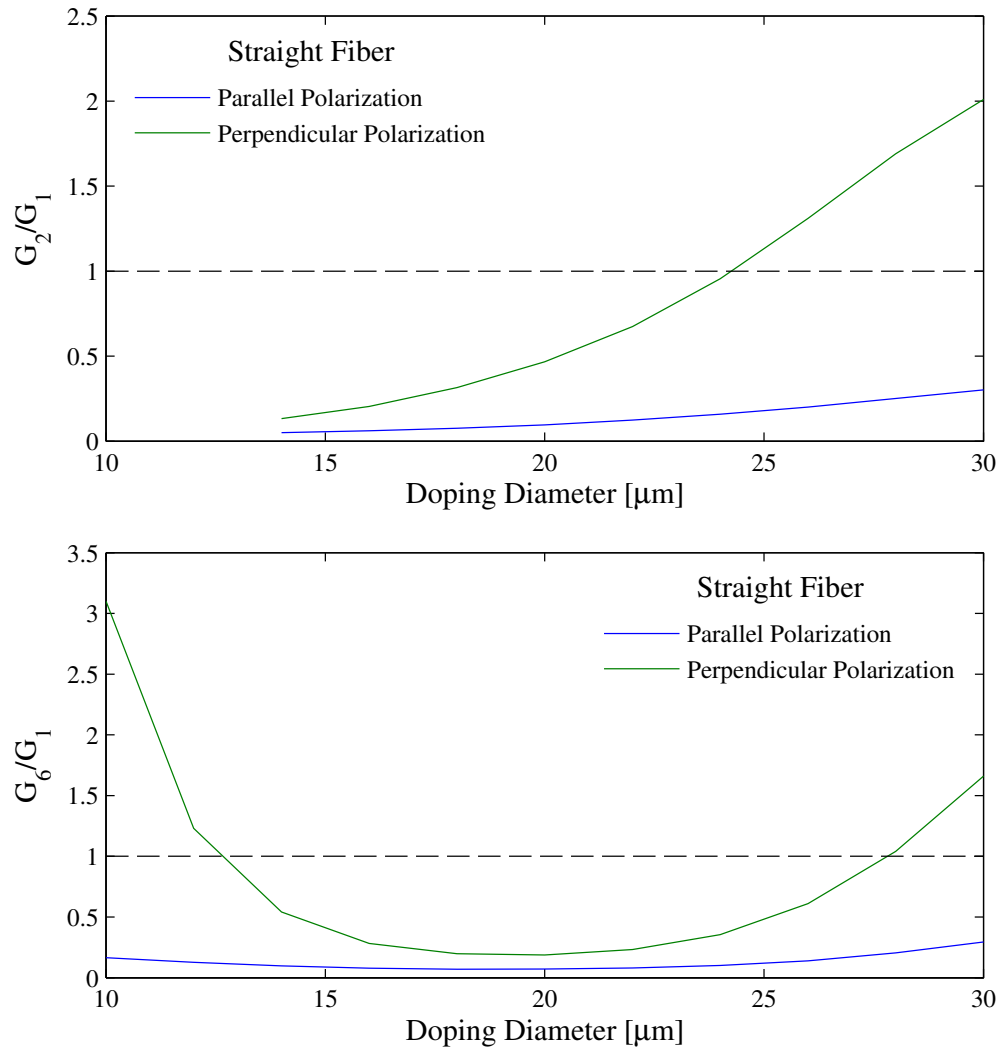


Fig. 5. A comparison of the relative gains vs. doping diameter for co-pumping. Other parameters are listed in Table 1. The gain G_m is the output power divided by the input power in the m^{th} mode. The upper plot is the gain of modes $m_{2\perp}$ and $m_{2\parallel}$ relative to m_1 ; the lower is the gain of modes $m_{6\perp}$ and $m_{6\parallel}$ relative to m_1 . For non-PM fiber the gain of mode 2 is reasonably approximated by the geometric mean of the two curves shown.

Fig. 6 summarized our results for a similar calculation using fiber bent to a 50 mm radius. Bending increases the gains of m_2 and m_6 of both polarizations relative to m_1 . The ratio of

powers for the two polarizations of m_2 and m_6 is approximately the same as in unbent fiber, and the effect of confined doping is also similar.

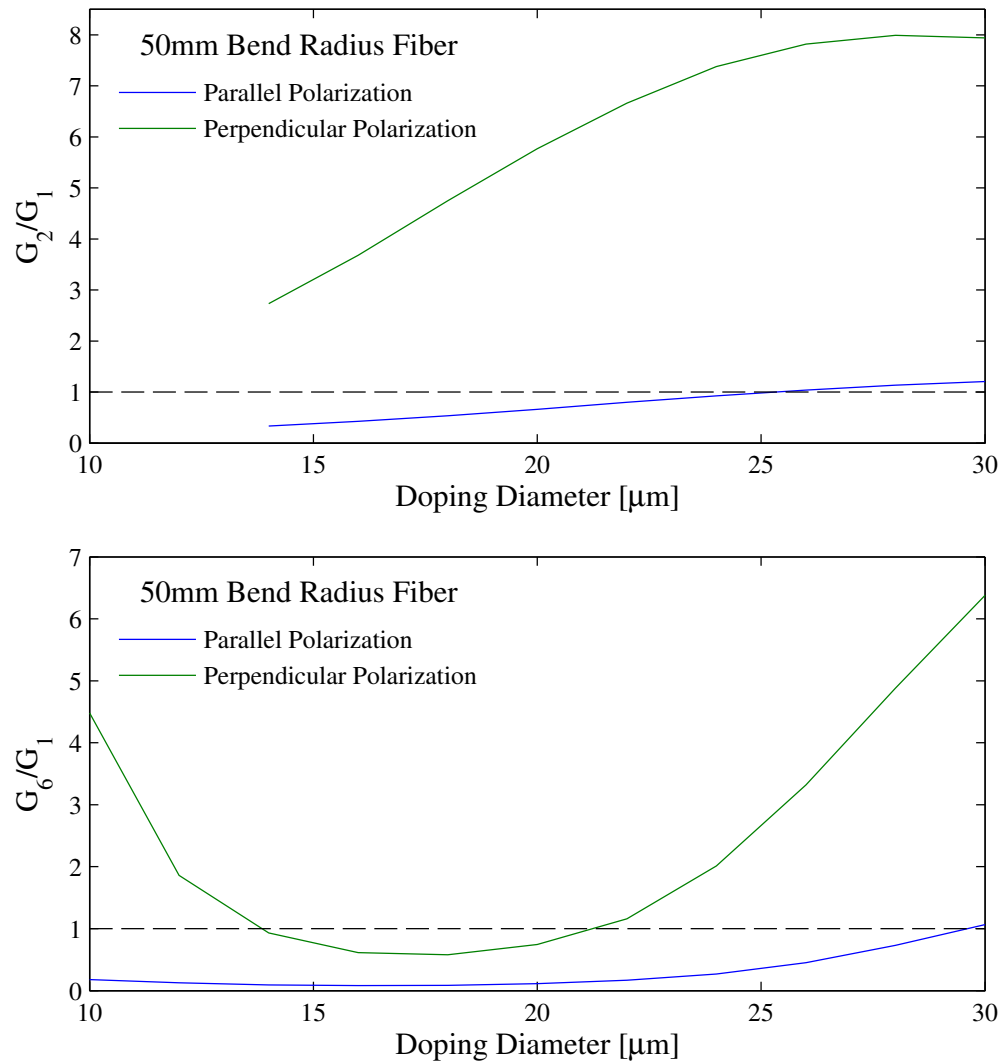


Fig. 6. A comparison of the relative gain vs. doping diameter for fiber bent to a radius of 50 mm in co-pumped amplifier (see Fig. 1 for bent fiber mode profiles). Other parameters are listed in Table 1. The gain G_m is the output power divided by the input power in the m^{th} mode. The upper plot is the gain of modes $m_{2\perp}$ and $m_{2\parallel}$ relative to m_1 ; the lower is the gain of modes $m_{6\perp}$ and $m_{6\parallel}$ relative to m_1 . For non-PM fiber the gain of mode 2 is reasonably approximated by the geometric mean of the two curves shown.

5. Discussion

In the results presented here we have used 1% of the total power in the higher order mode. However, our modeling shows that the degree of suppression is quite constant for higher power ratios, up to 25% power in the higher order mode. Further, if several higher order modes are

populated at the 1% level we find each interacts with the fundamental mode nearly independently, and each is suppressed as though the other modes were absent.

We note that the fundamental mode is not unique in creating a differential gain between the two polarizations of a much weaker mode. It appears that any strong mode can produce this effect on any weak mode.

6. Conclusions

In coherent beam combining a pure fundamental (LP_{01}) mode is desired from each fiber amplifier. The second mode (LP_{11}) probably poses the biggest problem because it adds variable uncorrected tilts to the beam which degrades efficiency of the combination process. This mode is also easily populated at launch by slight tilts and displacements of the amplifier fiber relative to the input beam. Only the light in LP_{11} polarized parallel to the fundamental at the output end is of real concern because the orthogonally polarized light, while it wastes a certain amount of pump power, does not interfere with beam combination.

As we have demonstrated, in a PM fiber the parallel polarized light of the non-dominant mode is substantially suppressed by gain saturation. Differential gain between the fundamental and higher order modes due to mode competition does not worsen the beam quality as is sometimes claimed, but rather helps purify the output beam. In non-PM fiber the polarizations of the fundamental and higher order mode do not evolve together, so at the fiber output the power in a higher order mode is on average nearly equal in the two polarizations, and its power is intermediate between the suppressed and enhanced levels. Here again, however, mode competition does not degrade mode purity. Only in tightly bent fiber does the mode purity degrade due to mode competition.

If greater suppression of higher order modes is required than is available from the mode competition effect, confined doping can be used. We have shown that this suppression adds with that provided by competition. However, confined doping may be incompatible with tight bending.

The overall conclusion must be that the effects of mode competition on beam quality from high power fiber amplifiers are modest, and except for tightly bent fiber are unlikely to strongly impact the beam quality. However, it is noteworthy that to the extent it does have an influence, it is usually positive, contradicting the notion of degradation due to mode competition. In any case, we have demonstrated that the effects can be modeled realistically in reasonable run times, so further exploration through modeling is straightforward.

Finally we note the well known method of bending the fiber to smaller radii than we used can be an effective way to suppress higher order modes. The differential bend loss between the fundamental and higher order modes may be sufficient to suppress higher order modes without excess loss of the fundamental [17]. Done properly, this can have a much stronger influence on beam quality than does mode competition.